A geometrical formulation of the μ-lower bound problem ⋆

Jongrae Kim*, Declan G. Bates†, Ian Postlethwaite‡

Control & Instrumentation Research Group, Department of Engineering, University of Leicester, Leicester LE1 7RH, UK

* *jkim@aero.gla.ac.uk,* † *dgb3@leicester.ac.uk,* ‡ *ixp@leicester.ac.uk*

Abstract

A new problem formulation for the structured singular value μ in the case of purely real (possibly repeated) uncertainties is presented. The approach is based on a geometrical interpretation of the singularity constraint arising in the μ lower bound problem. An interesting feature of this problem formulation is that the resulting parametric search space is independent of the number of times any parameter is repeated in the structured uncertainty matrix. A corresponding lower bound algorithm combining randomisation and optimisation methods is developed, and some probabilistic performance guarantees are derived. The potential usefulness of the proposed approach is demonstrated on two high-order real μ analysis problems from the aerospace and systems biology literature.

1 Introduction

μ-analysis has become a widely used approach for the robustness analysis of uncertain linear time-invariant systems. The structural singular value, μ, is defined as the inverse of the magnitude of the smallest uncertainty, from a defined set, which makes the corresponding system unstable. The exact value of μ is rarely computed in practice because of fundamental numerical difficulties, but upper and lower bounds on μ can usually be calculated, [1,17]. Upper bounds on the structured singular value (μ) in the case of purely real uncertainties can generally be computed without difficulty by applying the standard upper bound algorithms developed for the case of mixed real and complex uncertainties, e.g. [1]. While computational experience suggests that the resulting upper bounds are usually quite tight, it is known that for problems involving repeated uncertain parameters, in particular, the upper bound can be

⋆ The first author is now with the Department of Aerospace Engineering, University of Glasgow, Glasgow G12 8QQ, UK. This work was carried out under EPSRC research grant GR/S61874/01.

arbitrarily conservative, [1,19]. For this reason, it is highly desirable to be able to also compute tight lower bounds for the real μ problem. Unfortunately, computation of the μ lower bound in the case of purely real uncertainties is a well known NP-hard problem [8,9]. In fact the first, and best known, algorithm for computing real μ lower bounds is exponential time, [3], which for practical purposes limits its application to analysis problems involving up to approximately 14 uncertain parameters. An alternative approach, proposed in [5], extracts the real part of the smallest destabilising mixed real/complex uncertainty (which can be computed in polynomial time), and scales this up until an eigenvalue of the closed-loop system crosses the imaginary-axis. In contrast to the algorithm of [3] which computes a μ lower bound over a grid of frequencies, this approach computes an estimate of the peak of the lower bound (in fact a skewed-μ lower bound). Furthermore, neither of the above approaches are applicable to systems with repeated uncertain parameters, [4].

Two other approaches for computing lower bounds on μ for problems with large numbers of uncertain real parameters are described in [11]. The first uses μ sensitivities to try to identify which (if any) uncertain parameters may be discarded so that the dimension of the problem can be reduced to a size for which the algorithm of [3], may be applied. The second formulates the lower bound calculation as a constrained optimisation problem which may be solved (suboptimally) using standard numerical optimisation software. While these approaches can handle repeated parameters and were shown in [11] to allow the computation of reasonable bounds for a realistic robustness analysis problem, they are again likely to be of limited use for general high-order problems. Finally, an "engineering fix" for the real μ lower bound problem is the so-called regularisation approach - small amounts of complex uncertainty are added to each real parameter so that the problem becomes a mixed μ problem, [1,10] and standard polynomial time algorithms can be applied. Significant drawbacks associated with this approach include (a) the real parts of the worst-case parameters computed for the regularised problem may be very far from the true worst-case values for the original real μ problem [4], and (b) it is no longer possible to use the lower bound to assess the level of conservatism in the original real μ upper bound.

In this paper, we present a new formulation of the real μ problem which appears to offer significant advantages for problems involving large numbers of (possibly repeated) uncertain parameters. The paper is organised as follows. In Section 2, a new geometrical interpretation of μ-analysis is presented and the advantages of this interpretation from a numerical and conceptual point of view are discussed. Section 3 discusses the development of solution algorithms for this problem formulation. In Section 4, the potential of the proposed approach is illustrated through its application to two high order real μ-analysis problems from the fields of flight control and systems biology. Section 5 presents

some conclusions. Details of the implementation of the computational algorithm used to solve the examples discussed in the paper are provided in Appendix I, while some some probabilistic performance guarantees for the algorithm are derived in Appendix II.

2 A Geometrical Interpretation of the Real μ Lower Bound Problem

The approach proposed in this paper is based on a geometrical analysis of the subset in the uncertain parameter space that satisfies the singularity constraint arising in the μ lower bound computation:

$$\det\left[I - M(j\omega)\Delta\right] = 0 \tag{1}$$

where $\det(\cdot)$ is the determinant of the matrix, I is the identity matrix whose size corresponds to the size of $M(j\omega)\Delta$, $M(j\omega)$ is a system transfer function matrix representing the "known" part of the system, j is the imaginary number, i.e. $\sqrt{-1}$, ω is a non-negative real number in $\mathbb{R}$, i.e. frequency, Δ is a diagonal matrix of uncertain norm-bounded real parameters, which may be repeated, and $\mathbb{R}$ is the set of real numbers. Since the value of the determinant in (1) is complex in general, the singularity condition can be written in terms of its real and imaginary parts as:

$$f_R(\Delta) \equiv \Re\left\{\det\left[I - M(j\omega)\Delta\right]\right\} \tag{2a}$$

$$f_I(\Delta) \equiv \Im\left\{\det\left[I - M(j\omega)\Delta\right]\right\} \tag{2b}$$

where $\Re(\cdot)$ and $\Im(\cdot)$ are the real and the imaginary parts of the argument, respectively, and Δ is an element of the following set, i.e. $\Delta \in \mathbf{\Delta}$, [17]:

$$\mathbf{\Delta} = \left\{\mathrm{diag}\left[\delta_1 I_{r_1},\, \delta_2 I_{r_2},\, \ldots,\, \delta_p I_{r_p}\right] \;\middle|\; \delta_i \in \mathbb{R}\right\} \tag{3}$$

where diag[...] is the diagonal matrix whose elements are given as arguments, r_i is an element of the set $\mathbb{N}$, the positive integers, and I_{r_i} is the $r_i \times r_i$ identity matrix for $i = 1, 2, \ldots, p$. Note that the number of uncertain parameters is p, and each uncertain parameter δ_i is repeated r_i times, where r_i may be 1. Now, the singularity condition, (1), is written as the intersection of the following two sets or manifolds (submanifolds in $\mathbb{R}^p$):

$$F_R = \{\Delta \in \mathbf{\Delta} | f_R(\Delta) = 0\} \tag{4a}$$

$$F_I = \{\Delta \in \mathbf{\Delta} | f_I(\Delta) = 0\} \tag{4b}$$

and μ is defined by

$$\mu \equiv \begin{cases} \dfrac{1}{\min_{\Delta \in F_R \cap F_I} \bar{\sigma}(\Delta)}, & \text{if } F_R \cap F_I \neq \emptyset \\ 0, & \text{otherwise} \end{cases} \tag{5}$$

For $\Delta = 0$, the determinant (1) is equal to one, and therefore $f_R(0) = 1$ and $f_I(0) = 0$. Hence, the manifold F_I always passes through the origin and the manifold F_R is always away from the origin with a strictly positive distance. Note that the singularity conditions (4) must be checked for each frequency, ω, which is an element of $[0, \infty)$. In practice, a certain range of frequencies is gridded into a finite number of points and μ is estimated for each point. In this paper, we frequently refer to these manifolds as curves or surfaces when the surrounding space, i.e. $\mathbb{R}^p$, p-dimensional Euclidean space, is of two or three dimensions. Moreover, if no confusion arises, we sometimes call a manifold simply a curve or a surface. Whenever either F_R or F_I is empty, the lower bound for μ is equal to zero. Thus for well-motivated problems we can assume neither F_R nor F_I are empty, and they can thus be treated as two surfaces, i.e., two $(p-1)$-dimensional submanifolds, $\mathbb{R}^{p-1}$ in $\mathbb{R}^p$. When p is equal to two, for example, two possible singularity situations are shown in Fig. 1. Since the submanifold where the two constraints are satisfied is the intersection of two sets, F_R and F_I, i.e. $F_R \cap F_I$, it is a $(p-2)$-dimensional submanifold, $\mathbb{R}^{p-2}$. As shown in Fig. 1, when p is equal to two, it is a point. Obviously, it is of measure zero in $\mathbb{R}^p$ space and therefore the probability of any randomisation-based search procedure finding this feasible solution set (i.e. not a tight lower bound but *any* lower bound) is zero in this case.

However, by inspecting the submanifolds in Fig. 1, which satisfy the constraints, (4), the following can be deduced. Consider a small box, with the length of each edge (edge in two-dimensional space, face of a hyper-box in higher dimensional space) equal to a fixed ∞-norm, around the singular region, for example, the two boxes in Fig. 1. The difference between the singularities in boxes $\mathbf{A}_1$ and $\mathbf{A}_2$ is due to the angle between the two tangential planes at the singular point. The angle between the two tangential planes inside $\mathbf{A}_1$ is zero whereas the angle inside $\mathbf{A}_2$ is non-zero. Note that if the angle is non-zero, there are four sign combinations of the real and imaginary parts of the determinant inside the box. If the angle is zero, there are three sign combinations. In this paper we aim to find the singularity case of $\mathbf{A}_2$ rather than the one of $\mathbf{A}_1$. Assuming that the angle between the tangential planes is greater than a certain number, the area of each of the four regions containing the four possible sign combinations will also be greater than a certain volume. Then, since these four regions have the same dimension as the uncertain space, $\mathbb{R}^p$, the probability of finding these regions by a randomisation-based search is non-zero (unlike the probability of finding the singular submanifold itself, which is zero).

3 Solution of the Geometrical Problem Formulation

Several possible approaches could be employed to generate solutions for the proposed real μ lower bound problem formulation. Consider, for example, two boxes centred at the origin in the uncertain parameter space (these will be hyper-boxes in higher dimensional space) as shown in Fig. 2. If we randomly select points along the edges of the box (faces of the hyper-box) $\mathbf{B}_1$, and evaluate the signs of f_R and f_I, we will find at most two combinations, i.e., sign(f_R, f_I) = (1, 1) or (1, −1). On the other hand, for the larger box, $\mathbf{B}_2$, the maximum possible number of sign combinations is four, i.e., sign(f_R, f_I) = (1, 1), (1, −1), (−1, 1), or (−1, −1). Therefore, there is an intersection of two submanifolds, which satisfies the singularity constraint, inside this box. In this case, the calculation of the μ-lower bound is very simple because we only need to check each edge of the box to find the four sign combinations. If they are not found, we increase the size of the box and check the signs again (for a discussion of efficient approaches for incrementing the size of the hyper-box, see Appendix I). This process is repeated until the four sign combinations are found, and then the maximum magnitude of the hyper-box gives the lower bound on μ. The search procedure described above relies on each of the two submanifolds being continuous and connected. The submanifolds generated by the singularity constraints are obviously continuous in terms of Δ, however, they are not connected, in general. This can be seen by considering the following example from [9], where:

$$M = \begin{bmatrix} 0.3846 + 1.9231j & 0.0769 + 1.3846j \\ 0.3846 + 1.9231j & -1.9231 + 0.3846j \end{bmatrix} \tag{6}$$

and $\Delta = \text{diag}[\delta_1, \delta_2]$. For this problem, the singularity conditions (4) are given by

$$f_R(\Delta) = 1 - 0.3846\delta_1 + 1.9231\delta_2 + 1.1539\delta_1\delta_2 \tag{7a}$$

$$f_I(\Delta) = -1.9231\delta_1 - 0.3846\delta_2 - 4.2308\delta_1\delta_2 \tag{7b}$$

Clearly, when δ_1 and δ_2 are equal to zero, then $f_R(0)$ is 1 and $f_I(0)$ is 0. That is, the sign of f_R at the origin is always positive and the curve $F_I(\Delta)$ passes through the origin. The two curves are given by

$$F_R = \left\{ \Delta \in \mathbf{\Delta} \;\middle|\; \delta_2 = \frac{2(-5000 + 1923\delta_1)}{19231 + 11539\delta_1} \right\} \tag{8a}$$

$$F_I = \left\{ \Delta \in \mathbf{\Delta} \;\middle|\; \delta_2 = \frac{-19231\delta_1}{2(1923 + 21154\delta_1)} \right\} \tag{8b}$$

and each of the curves is disconnected and forms two separate curves, respectively. The difficulty that arises for the proposed geometrical approach as a result of the possible disconnectedness of the surfaces is that we have to discard the luxury of just checking the signs of all edges of the box (in the higher-dimensional space, faces of the hyper-box) to obtain the lower bound. Instead, a hyper-box, whose radius is small enough such that the possible disconnection of the surfaces is avoided, is placed around the candidate intersection region. Some random points are uniformly spread *inside* the hyper-box and if not all sign combinations are found, then the size of the box is incremented - see Appendix I for a full discussion and algorithmic implementation.

4 Example Applications

4.1 Robustness Analysis of a Flight Control Law

The first example used to illustrate the advantages of the proposed geometric problem formulation involves the robustness analysis of a flight control law for a civil transport aircraft. The aircraft model has 14 non-repeated real uncertain parameters representing uncertainty/variations in its aerodynamic parameters, [4]. This type of real μ-analysis problem is typical of the kind that arises in the industrial clearance process for flight control laws in both civil and military aircraft, [7]. The upper and lower bounds on μ computed for this problem are shown in Fig. 3. Lower bounds were computed using the algorithm of [3], the peak lower bound algorithm of [5,6] and the proposed algorithm. All three algorithms produced almost exactly the same peak value of the lower bound, i.e. 0.18. Compared to the algorithm of [3], the approach proposed in this paper delivers a very similar lower bound but in a dramatically shorter time: 3.85 hours for 258 frequency points (approx. 53.67 sec per point) versus 29.40 hours (approx. 6.84 minutes per point) for the algorithm of [3]. The rather jagged nature of the lower bound shown in the first subplot of Fig. 3 can easily be improved by adjusting various parameters in the algorithm, at the cost of some increase in computation time. By increasing the computation time by about 9 hours, for example, the quality of the lower bound is significantly improved as shown in the second plot in Fig. 3. In Fig. 4, computation times for the new algorithm and the Dailey's algorithm [3] are compared for varying numbers of uncertain parameters.

4.2 Robustness Analysis of a Biochemical Network Model

For the second example application, the robustness of a recently proposed mathematical model for the biochemical network producing internal cAMP (cyclic Adenosine Monophosphate) oscillations in *Dictyostelium discoideum* is considered, [13]. Robustness analysis has recently become a subject of crucial importance in the field of Systems

Biology, since it can provide a means of validating (or invalidating) proposed models of biological systems which have been shown experimentally to be robust to variations in their environment. In [12,14] it was shown how the original form of the model proposed in [13] could be converted to the standard linear fractional transformation (LFT) form so that μ-analysis tools could be used to evaluate its robustness. The resulting uncertainty model contains 13 real uncertain parameters, each of which is repeated 39 times (the dimension of the uncertainty matrix Δ is thus 507×507). Due to the large number of highly repeated uncertain parameters, in previous analysis of this model (see [12,14]) only an upper bound on the value of μ could be computed. This is highly problematic, since as shown in Fig. 5, the upper bound on μ computed for this problem is very large, suggesting a (possible) extreme lack of robustness for this model. Using the approach proposed in this paper, a quite reasonable lower bound for this problem could be computed, as shown in Fig. 5. A frequency gridding of 48 points was used, and the peak value of the lower bound was computed as 723.56. This result establishes beyond doubt the extreme lack of robustness of the proposed network model. The calculation time for the lower bound was approx. 66.07 hours, or 1.38 hours per frequency point. Note that neither the algorithm of [3] or [5,6] could be applied to the above problem, since it contains repeated real uncertain parameters.

5 Conclusions

A new approach for calculating lower bounds on μ in the case of purely real and possibly repeated uncertain parameters was presented. The approach is based on insight gained from a novel geometric interpretation of the real μ lower bound problem, and is ideally suited to problems involving large numbers of uncertain parameters. In particular, it can be applied to problems involving repeated real uncertainties, for which very few practically useful methods currently exist in the literature. A computational algorithm was developed for the proposed problem formulation and successfully applied to two extremely challenging high-order real μ analysis problems from the aerospace and systems biology literature.

A Appendix I: Implementation of a computational algorithm

Incrementing the size of the hyper-box:

Increasing the amount by which the size of the hyper-box is increased (or decreased) at each step of the algorithm will reduce the computation time, but will also reduce the tightness of the μ lower bound. For example, if the increase in the size of the hyper-box is too large, i.e., from $\mathbf{B}_1$ to $\mathbf{B}_2$ in one step, then we will miss the singular points that are closer to the origin (e.g. s_1 or s_2 in Fig. 2), which correspond to tighter μ lower bounds than the one for s_3. On the other hand, if we increase the size of the hyper-box by a small amount at each step, we will have a higher probability of finding a tighter μ-lower bound, but with the expense of increasing the computation time. To avoid having to use very small increments in the size of the hyper-box, the following property of the two surfaces $f_R(\Delta) = 0$ and $f_I(\Delta) = 0$ can be exploited: if Δ equals zero, the determinant of $I - M(j\omega)\mathbf{0}$ equals 1 for all ω in $[0, \infty)$. Hence, $f_R(0) = 1$ and $f_I(0) = 0$. Geometrically, the surface $f_I(\Delta) = 0$ is passing through the origin in the uncertain space and the surface $f_R(\Delta) = 0$ is away from the origin and thus the sign of $f_R(\Delta) = 0$ around the neighbourhood of the origin is positive. Since we know that $f_R(0) = 1$ and $f_I(0) = 0$, for any algorithm starting to search from the neighbourhood of the origin, the following two sign combinations can be found immediately : sign(f_R, f_I) = (1, 1) or (1, -1). In this "*exploration*" stage of the algorithm, a certain number of random points are spread on the surface of the hyper-box, and if all four sign combinations are not found, the size of the hyper-box is increased. Hence, the following two sign combinations are found last among the four combinations: sign(f_R, f_I) = (-1, 1) or (-1, -1). However, since the increment in the size of the hyper-box is discrete, the following minimisation problem can be formulated and solved (locally) immediately after the four sign combinations are found to reduce the gap between the size of the current hyper-box and the location of the true singular point:

$$\min_{\Delta \in \mathbf{\Delta}} J = \bar{\sigma}(\Delta) \tag{A.1}$$

subject to

$$f_R(\Delta) < 0 \tag{A.2a}$$

$$f_I(\Delta) < 0 \text{ or } f_I(\Delta) > 0 \tag{A.2b}$$

$$\bar{\sigma}(\Delta) \leq \bar{\sigma}(\Delta^k) \tag{A.2c}$$

where the second constraint is chosen depending on which sign of $f_I(\Delta^k)$ was found last and Δ^k is the uncertain matrix at the last step. This optimisation step allows the use of larger increments in the size of the hyperbox and thus reduces the overall computation time for the algorithm. For the results presented in this paper, we used the *fmincon* function in the MATLAB optimisation toolbox, [15], which uses SQP (Sequential Quadratic Programming).

The problem of disconnected submanifolds:

Since each submanifold could be disconnected as shown in Fig. 6, in order to make sure that when four sign combinations are found they actually occur because of the intersection of two hyper-surfaces, we proceed as follows. Let Δ_0^* in Fig. 7 be the random point having the sign combination that is found last in the *exploration* step of the algorithm. This is the starting point of the *minimisation* step which tries to reduce the distance from the origin, O, subject to the sign constraints given in (A.1). Let Δ_1^* be the solution from the minimisation step. As shown in Fig. 7, although it reduces the distance from the origin, it actually moves away from the actual singular points. Now, the *expansion & contraction* step of the algorithm is applied: A hyper-box, whose radius is small enough such that the possible disconnection of the surfaces is avoided, is placed around the candidate intersection region whose centre is Δ_1^*. Some random points are uniformly spread *inside* the hyper-box and if not all sign combinations are found, then the size of the box is increased. For example, the size of the box keeps increasing from $\mathbf{B}_1^0$ until $\mathbf{B}_1^{k_1}$. Because of the smallest area compared to the areas having other sign combinations for $\mathbf{B}_1^{k_1}$, the last point, Δ_2^*, will be most likely inside the region Ar_1. Then, a hyper-box is centred at Δ_2^* and the same procedure is applied. In the next stage a new hyper-box may be placed at Δ_3^*. By reducing the size of the hyper-box and moving its centre in this way, the true intersection will be enclosed by the box. Then, the lower bound is the maximum value of the absolute values of all Δ, which are generated by inspecting the sign combinations on the hyper-box. This is the most computationally expensive part of the proposed algorithm.

Main steps in the algorithm (full MATLAB implementation available on request from the first author):

(1) **Exploration**: Check the sign of $f_R(\Delta_i)$ and $f_I(\Delta_i)$ for uniform random samples Δ_i on the faces of a hyper-box centred at the origin in the uncertain space, until either the maximum number of samples is reached or the four sign combinations are found. If the combinations are not found, increase the size of the hyper-box.

(2) **Minimisation**: Solve locally the optimisation problem, (A.1).

(3) **Expansion & Contraction**: In Fig. 7 initially the centre of the box will be at Δ_1^*, which is either the solution of (A.1) or the last Δ, which gives the last sign combination in the **Exploration**. The four sign combinations may be found when the size of the box is increased up to $\mathbf{B}_1^{k_1}$. Probabilistically, the last sign combination coming from the region Ar_1 and the new hyper-box centre will be at Δ_2^*. Repeating the same operation may give the next centre at Δ_3^* which is inside the region Ar_2. Then, the centre of the box will approach the singular region and this procedure is repeated until the size of the box is smaller than some tolerance value.

B Appendix II: Computational Complexity and Performance Guarantees

Since the number of operations for computing the determinant of an $n \times n$ matrix is in the order of $n^3/3$ [16], the upper bound for the total number of operations to compute the μ lower bound at each frequency point ω using the suggested approach is approximately given by

$$\frac{n^3}{3}\left(k\bar{N} + \bar{N}_{\text{opt}} + \frac{\bar{N}}{10}\bar{N}_{\text{ec}}\right) \tag{B.1}$$

where each term inside the parentheses from left to right is the maximum number of operations for each stage of the algorithm, i.e. *Exploration*, *Minimisation*, and *Expansion & Contraction*. The value of k is the number of steps in the *Exploration* stage required to find the four sign combinations, $\bar{N}$ is the maximum number of sample points for the *Exploration* stage, $\bar{N}_{\text{opt}}$ is the maximum allowed number of function evaluations for the optimisation routine in the *Minimisation* stage, and finally the number of operations for the *Expansion & Contraction* stage is given by the last term, where the maximum number of samples for a given hyper-box is chosen to be a tenth of $\bar{N}$ and the maximum iteration is N_{ec}. If the frequency range over which the lower bound is to be computed is gridded into N_ω points, then the upper bound of the total number of operations required to obtain the real μ lower bound is given by

$$N_\omega\left[\frac{n^3}{3}\left(k\bar{N} + \bar{N}_{\text{opt}} + \frac{\bar{N}}{10}\bar{N}_{\text{ec}}\right)\right] \tag{B.2}$$

Thus the computational cost of the proposed algorithm increases polynomially with the dimension of determinant, n.

Since the real μ lower bound problem is itself NP-hard, there will always be some cases for which any non-exponential-time algorithm fails to return a solution, [18]. To get a feeling for how likely this is to occur in practice, we develop some general probabilistic guarantees of performance for the proposed algorithm using the Chernoff bound, [2]. which

is defined as follows: if the number of samples, N, satisfies the following inequality:

$$N \geq \frac{1}{2\epsilon^2} \log \frac{2}{\delta} \tag{B.3}$$

then the following inequality is also satisfied:

$$\text{Probability}\left\{|p(r_\infty) - \hat{p}_N(r_\infty)| \leq \epsilon\right\} \geq (1 - \delta) \tag{B.4}$$

for $\epsilon \in (0,\, 1)$ and $\delta \in (0,\, 1)$ where

$$p(r_\infty) = \text{Probability}\left\{\text{sign}[f_R(\Delta^i),\, f_I(\Delta^i)] = A \text{ on the face of hyper-box whose size is } r_\infty\right\} \tag{B.5}$$

Here, A equals one of the sign combinations, $(1,\, 1)$, $(1,\, -1)$, $(-1,\, 1)$, or $(-1,\, -1)$, the empirical probability is given by

$$\hat{p}_N(r_\infty) = \frac{1}{N} \sum_{i=1}^{N} I(\Delta^i) \tag{B.6}$$

where Δ^i is an element of the set, $\left\{\Delta^i | \bar{\sigma}(\Delta^i) = r_\infty\right\}$, i.e. it is a point on the face of the hyper-box whose radius is of ∞-norm r_∞, and the indicator function is as follows:

$$I(\Delta^i) = \begin{cases} 1, & \text{if sign}[f_R(\Delta^i),\, f_I(\Delta^i)] = A \\ 0, & \text{otherwise} \end{cases} \tag{B.7}$$

The inequality, (B.4), provides the information regarding the probability estimation error using a finite number of samples. Whenever the true probability $p(r_\infty)$ is estimated by a finite number of samples, which is given by $\hat{p}_N(r_\infty)$, where the number of samples, N, satisfies the Chernoff bound, then the estimation error satisfies the inequality, (B.4). ϵ and $(1 - \delta)$ represent the estimation error bound and the reliability of the bound [18]. Based on the above definitions, we can prove the following:

Theorem 1 *If the number of samples is equal to the Chernoff bound,* (B.3)*, and* $p(r_\infty)$ *satisfies*

$$p(r_\infty) \geq \frac{1}{N} + \sqrt{\frac{1}{2N} \log \frac{2}{\delta}} \tag{B.8}$$

then the probability of finding the region A on the face of the box for a given r_∞ *through the Exploration part of the algorithm is greater than* $(1 - \delta)$*.*

Proof. The proof is a straightforward application of the Chernoff bound and is omitted.

The *Expansion & Contraction* stage of the algorithm also delivers similar probabilistic performance to the *Exploration* part. The probability of trapping the actual singularity point depends, of course, on the number of evaluations for each box, $\bar{N}/10$, and on how many times this process is repeated, N_{ec}. Note, however, that there is currently no formal proof of convergence for this part of the algorithm. In the case that the algorithm does not converge in a given number of samples, the lower bound is declared as zero.

Finally, note that for the first example discussed in the paper, we chose $\bar{N} = 2000$ so that the smallest $p(r_\infty)$ given by (B.8) is 4.12% with $\delta = 0.0023$ (3σ bound). Hence, whenever the smallest portion of the sign combinations among the four possibilities is greater than 4.12%, the four sign combinations are guaranteed to be found with a probability greater than $(1 - \delta)^4 = 98.96\%$. For the second example, we chose $\bar{N} = 1000$ so that the smallest $p(r_\infty)$ given by (B.8) is 5.86% with $\delta = 0.0023$ (3σ bound). As a result, whenever the smallest portion of the sign combinations among the four possibilities is greater than 5.86%, the four sign combinations are guaranteed to be found with a probability greater than 98.96%.

References

[1] G. J. Balas, J. C. Doyle, K. Glover, A. Packard, and R. Smith, *μ-Analysis and Synthesis Toolbox: For Use with MATLAB, User's Guide, Version 3.* The MathWorks, Inc., 2001.

[2] H. Chernoff, "A measure of asymptotic efficiency for tests of a hypothesis based on the sum of observations," *The Annals of Mathematical Statistics*, vol. 23, no. 4, pp. 493–507, Dec. 1952.

[3] R. L. Dailey, "A new algorithm for the real structured singular value," in *Proceedings of the American Control Conference.* NY, USA: Inst. of Electrical and Electronics Engineers, 1990.

[4] G. Ferreres, *A Practical Approach To Robustness Analysis With Aeronautical Applications.* Kluwer Academic/Plenum Publishers, 1999.

[5] G. Ferreres and J. M. Biannic, "Reliable computation of the robustness margin for a flexible aircraft," *Control Engineering Practice*, vol. 9, pp. 1267–1278, 2001.

[6] ——, "Skew mu toolbox : a presentation," ONERA, Toulouse, France," Technical Report, August 2003. [Online]. Available: http://www.cert.fr/dcsd/idco/perso/Ferreres

[7] C. Fielding, A. Varga, S. Bennani, and M. S. (Eds.), *Advanced Techniques for Clearance of Flight Control Laws*. Springer, 2002.

[8] M. Fu, "The real structured singular value is hardly approximable," *IEEE Transaction on Automatic Control*, vol. 42, no. 9, pp. 1286–1288, Sept. 1997.

[9] M. Fu and S. Dasgupta, "Computational complexity of real structured singular value in l_p setting," *IEEE Transaction on Automatic Control*, vol. 45, no. 11, pp. 2173–2176, Nov. 2000.

[10] S. L. Gatley, D. G. Bates, M. J. Hayes, and I. Postlethwaite, "Robustness analysis of an integrated flight and propulsion control system using μ and the ν-gap metric," *Control Engineering Practice*, vol. 10, no. 3, pp. 261–275, Mar. 2002.

[11] M. J. Hayes, D. G. Bates, and I. Postlethwaite, "New tools for computing tight bounds on the real structured singular value," *Journal of Guidance, Control, and Dynamics*, vol. 24, no. 6, pp. 1204–1213, November-December 2001.

[12] J. Kim, D. G. Bates, I. Postlethwaite, M. Lan, and P. A. Iglesias, "Robustness analysis of biochemical networks using μ-analysis and hybrid optimisation," in *Proceedings of the joint 44th Conference on Decision and Control and European Control Conference*, Seville, Spain, December 2005.

[13] M. T. Laub and W. F. Loomis, "A molecular network that produces spontaneous oscillations in excitable cells of dictyostelium," *Molecular Biology of the Cell*, vol. 9, pp. 3521–3532, 1998.

[14] L. Ma and P. A. Iglesias, "Quantifying robustness of biochemical network models," *BMC Bioinformatics*, vol. 3, no. 38, 2002.

[15] MathWorks, *Optimization Toolbox (Version 2) For Use With MATLAB*. The MathWorks, Inc., 2003.

[16] ——, *MATLAB Function Reference*. The MathWorks, Inc., 2004, vol. 1: A-E.

[17] S. Skogestad and I. Postlethwaite, *Multivariable Feedback Control: Analysis and Design*. John Wiley & Sons Ltd., 1996.

[18] R. Tempo, G. Calfiore, and F. Dabbene, *Randomized algorithms for analysis and control of uncertain systems*. Springer-Verlag London, UK, 2005.

[19] P. Young, M. Newlin, and J. C. Doyle, "Practical computation of the mixed μ problem," in *Proceedings of the American Control Conference*, June 1992.

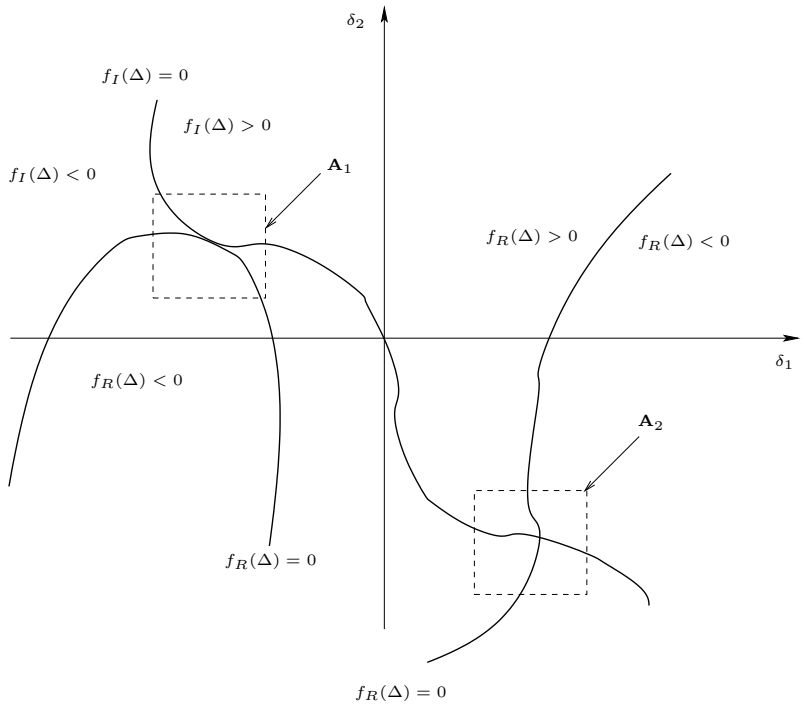

Fig. 1. Two topological possibilities that the intersection of two smooth surfaces, i.e. $F_R \cap F_I$, is not empty.

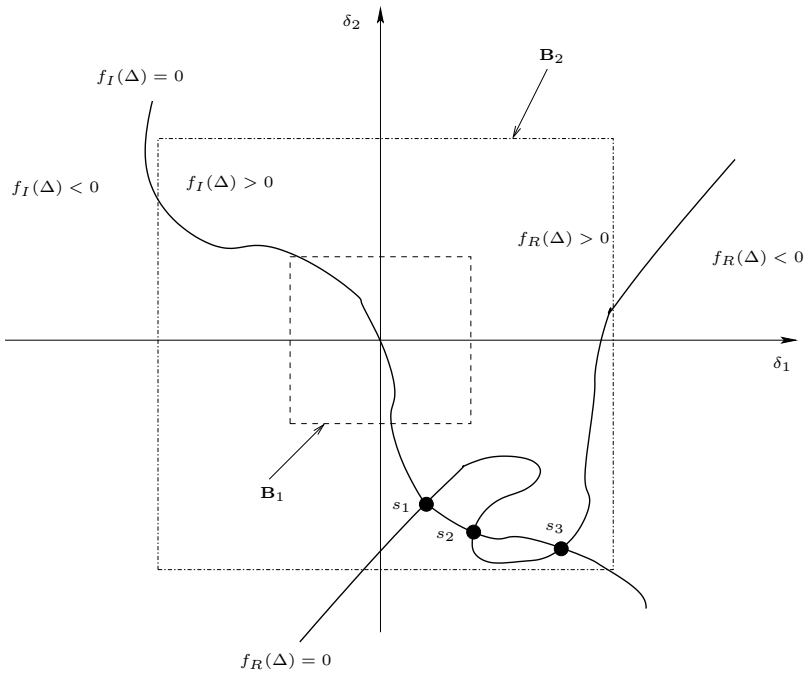

Fig. 2. Intersection of two surfaces where the matrix is singular

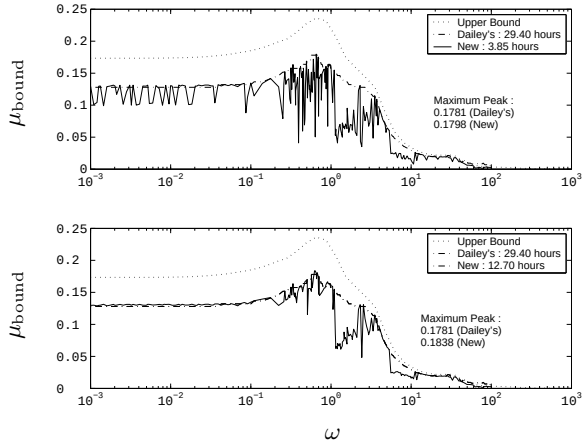

Fig. 3. μ upper and lower bounds for the rigid aircraft model

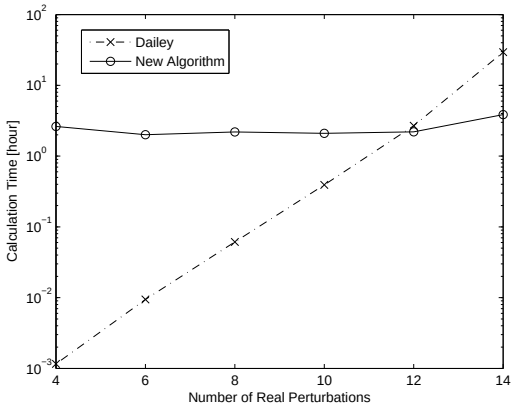

Fig. 4. Calculation time of algorithm for different sizes of the uncertainties

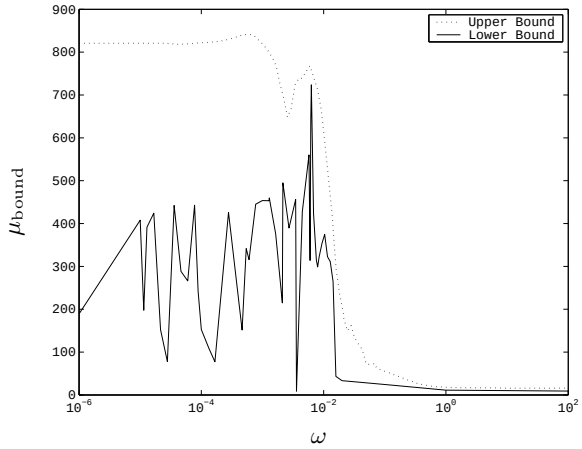

Fig. 5. μ upper and lower bounds for the bionetwork model

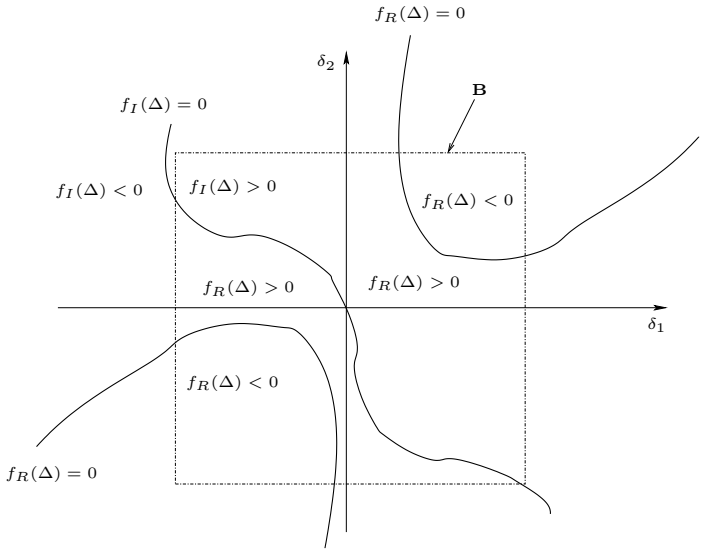

Fig. 6. Four sign combinations generated by disconnected surfaces

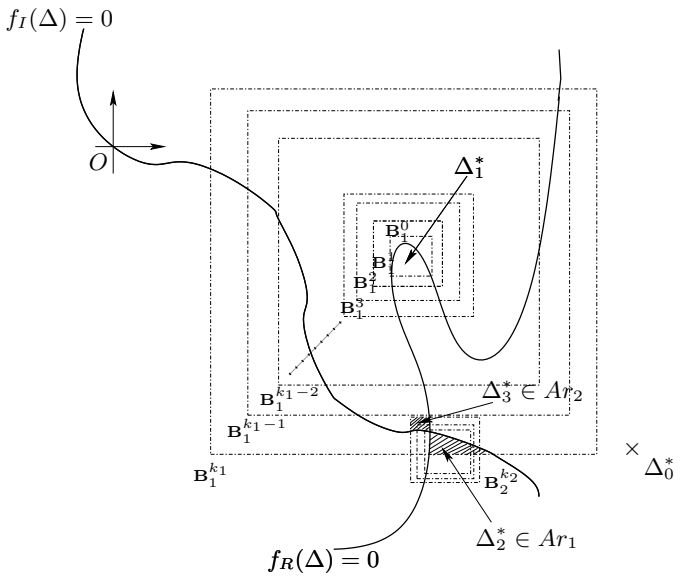

Fig. 7. *Expansion & Contraction* stage of the algorithm.